Energetics of stepped Cu surfaces

Z.-J. Tian*

*Institut für Grenzflächenforschung und Vakuumphysik, Forschungszentrum Jülich, D-5170, Jülich,
Federal Republic of Germany*

T. S. Rahman

Department of Physics, Kansas State University, Manhattan, Kansas 66506

We report here a systematic, computer simulation study of the energetics of stepped Cu(100) surfaces. With interatomic potentials described by the embedded-atom method we calculate multilayer relaxations, step-step interaction, step-kink formation energy, and the activation energies of adatoms diffusing on a series of stepped Cu(100) surfaces. The results affirm the existence of oscillatory and exponentially damped multilayer relaxations on $(1,1,n)$ vicinal surfaces. Furthermore, long-ranged step-step interaction is found to be present even for the short spacing of steps on the (1,1,3) surface. For the lower-index stepped surfaces the isolated step-pair interaction is found to be different from the ledge-ledge interaction. Comparisons are made of the kink-formation energy, step-step repulsion energy, and the activation energies with available experimental results and other calculations.

I. INTRODUCTION

An intriguing question in determining the equilibrium crystal surface structures[1] concerns the role that steps, kinks, and other defects play. These irregularities of vicinal surfaces impact a number of surface phenomena.[2] Stepped surfaces are also prone to roughening transitions and participate in the processes of evaporation, condensation, and melting. The proliferation of steps, their energetics, spacing, and the degree to which they meander on the surface are long-standing issues in statistical physics.[3-6] In recent years, there has been a resurgence of interest in the energetics and dynamics of vicinal (higher Miller index) surfaces due mainly to the availability of real-space imaging with the scanning tunneling microscope (STM), with which structural features of extended steps can be monitored and quantities like step energies, kink-formation energies,[9] kink concentrations,[7-11] and the activation energies of adatoms near the step edge[12] could be evaluated. These STM studies nicely complement the more traditional diffraction experiments with x rays or electrons of He beams, and have motivated several theoretical thermodynamical studies.[5,6]

The knowledge of the structure of the stepped surfaces is the first step toward the understanding of its characteristics. From a theoretical point of view, this structural information could be obtained by the crystal total-energy minimization procedures. For example, the stress relaxation on a Si(100) stepped surface was studied by atomistic calculations to identify the different types of elastic interactions,[13] while the "magic faceting" reconstruction on the Au(1,1,n) surfaces[14] has been examined from considerations of surface energies based on a many-body force model (glue model). Similarly, for Cu(113) and (115), an N-body, semiempirical potential was adopted to calculate multilayer relaxations, kink-formation energy, and step-step interactions.[15] Although good agreement with experiments was found for interlayer relaxations and

kink-formation energy, the model potentials used in Ref. 15 failed to reproduce the observed value of the elastic repulsive interactions between steps.

It is the purpose of this paper to apply a well-tested atomic interaction potential, i.e., that obtained by the embedded-atom method (EAM),[16] to examine the static properties and atomic mobilities of metallic vicinal surfaces, which to the best of our knowledge[17] have not as yet been explored. To this end we have carried out a systematic investigation of stepped surfaces Cu(1,1,n), with n varying from 3 to 99, which are all vicinal to Cu(100), and tabulated their surface energies, kink-formation energies, step-step interaction energy, multilayer relaxations, and the diffusional properties of adatoms along step edges and on terraces. It will be seen that the EAM potential is capable of reproducing the step-step elastic interaction, and that the activation energies of adatoms are also in reasonable agreement with experimental results. An interesting conclusion in the STM studies[9-11] of vicinal Cu(100) surfaces is the presence of attractive step-step interactions for intermediate distances of 3-5 atoms. We will comment on this in Sec. IV.

We will give a description of the model system in Sec. II, present the calculated results in Sec. III, and discussions in Sec. IV.

II. MODEL SYSTEM

The $(1,1,n)$ vicinal surface is realized by constructing a series of descending flat terraces of equal sizes along the x axis ([110]), with the normal along the z axis ([001]), as shown in Fig. 1. Note the $n = 2m + 1$, where m is an integer. For convenience, we take the nearest-neighbor distance between atoms $a_0/\sqrt{2}$ (a_0 being the lattice constant) as a unit length in this paper. The tilt angle between z', the normal of the $(1,1,n)$ surface, and z, the normal of the lower-index surface [001], is $\theta = \arctan(\sqrt{2}/2m + 1)$. Similarly, the step-step separa-
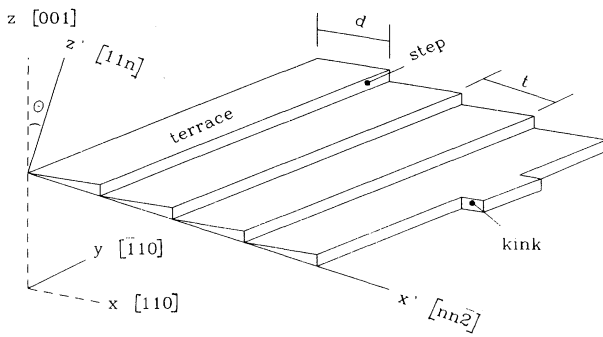
FIG. 1. The schematic of a $(1,1,n)$ stepped surface of a fcc metal. The step height is one monatomic layer thick.

tion $t = (\sqrt{2}\sin\theta)^{-1}$, while the terrace width d along [110] is $m + 1/2$. The monolayer step height is $h = \sqrt{2}/2$. As is obvious, the size of the terrace and, hence, m is controlled by the tilt angle θ.

The calculations of interest to us may be put in five categories involving (1) surface energy, (2) step-pair interaction, (3) kink-formation energy, (4) activation energies for adatom diffusion, and (5) surface relaxations. The calculation of the surface energy in turn also yields the step energy and the multilayer relaxation. In the simulations, the size of the supercell and the number of free surfaces to be modeled for the slab depend on several considerations—the guiding principle being that the system should be large enough to maintain the individuality of the steps, kinks, and adatoms, and yet be small enough to be tractable. Here the surface supercell of dimensions $N_{x'} \times N_{y'}$, where $N_{x'}$ is the number of terraces and $N_{y'}$ is the number of atoms along the step direction (y') chosen as follows. For the evaluation of the surface energy, the supercell is (4×4) in the case of the intermediate Miller index surface $(1,1,3)$ to $(1,1,9)$, i.e., those with $m = 1-4$, while it is a (2×4) supercell for $m = 5-49$. In the calculation of the kink-formation energy, $N_{y'}$ is increased to 12 while $N_{x'}$ remains the same as before. This assumes that the interaction between kinks along the step direction is negligible. The slab thickness N_x was taken to be 20 layers along [001], assuming that bulk behavior is obtained away from the surface. This slab has two identical free surfaces.

For calculations of the activation energies of adatoms on stepped surfaces, we found it more efficient to use a slab consisting of several dynamic layers placed on top of several static layers. Specifically, we used six dynamic and four static layers along [001]. The assignment of $N_{x'}$ and $N_{y'}$ was the same as that discussed above for the kink-formation energy.

Periodic-boundary conditions are applied along the surface plane (in the x' and y' directions), and the stepped structures are relaxed through energy minimization by the conjugate gradient method based on embedded-atom potentials. The EAM code used for this molecular-static (MS) technique is very similar to that applied earlier to study self-diffusion on Ag(111).[18] Results for energetics and the structure of these surfaces with defects are thus obtained and analyzed.

III. ENERGETICS OF $(1,1,2m+1)$ SURFACES

The characteristic energies of these vicinal surfaces may be put in four categories: surface/step energy, step-step interaction energy, kink-formation energy, and the activation energies of adatoms. By surface energy we mean the excess energy per unit area that the atom at the surface possesses, due to its lower coordination number, with respect to those in the bulk crystal. A related quantity, i.e., the step energy, is the difference in surface energy between the particular stepped surface and the flat (100) surface, and is so calculated. The step-step pair interaction, on the other hand, is the interaction energy between two isolated steps. The variation of this interaction energy is deduced from total-energy calculations using different microfacets on a (2×4) surface unit cell of $(1,1,99)$. Similarly, the kink-formation energy is the step-energy difference between a step with one kink and a straight step. Finally, the activation energy of adatoms is the potential barrier of an adatom jumping from one site to its neighbor site. Below, we present some details of these definitions.

A. Surface energies and ledge energies

The surface energy at $T = 0$ K stated above can be written as

$$\gamma(\theta) = \frac{E - N\epsilon_b}{2L_{x'}L_{y'}} , \tag{1}$$

where E is the total energy of the structure consisting of atoms obtained from the energy minimization, ϵ_b is the energy of a bulk atom, θ is the tilt angle as defined above, and $L_{x'}$ and $L_{y'}$ are the total lengths of the supercell along the x' and y' directions, respectively. The factor of 2 accounts for the two free surfaces of the slab used in the calculation. Thus $E-N\epsilon_b$ is the excess energy of the surface supercell.

The excess energy associated with a ledge (the step energy) is calculated similarly using the following expression:

$$\lambda(\theta) = \frac{E - N\epsilon_b - 2A_s\epsilon_u}{2N_{x'}L_{y'}} , \tag{2}$$

where $A_s = L_{x'}L_{y'}\cos\theta$ is the stepped surface area as projected onto the flat surface, and ϵ_u is the flat (100) surface energy. $N_{x'}$ is the number of terraces in the supercell. The factor of 2 takes into account the two free surfaces. The step energy $\lambda(\theta)$ and the surface energy $\gamma(\theta)$ thus have a simple relationship:

$$\gamma(\theta) = \epsilon_u\cos\theta + \lambda(\theta)\sin\theta/h , \tag{3}$$

where h is the step height.

The relaxed surface energies versus the tilt angle θ obtained from our simulations are shown in Fig. 2. As expected, the (111) surface is the most stable, while the (113) is the least so. Also, at small θ, i.e., when the steps are sufficiently rarefied and interact only weakly, the surface energy $\gamma(\theta)$ behaves like $\epsilon_u + k\theta$, where k is proportional to the isolated step energy. For selected surfaces,
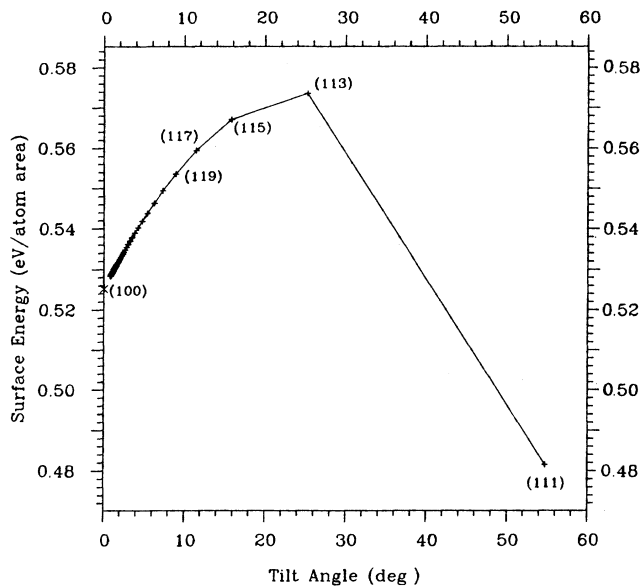
FIG. 2. The calculated surface energy per atom area $\gamma(\theta)$ with the step-tilt angle θ of $(1,1,n)$ vicinal surfaces.
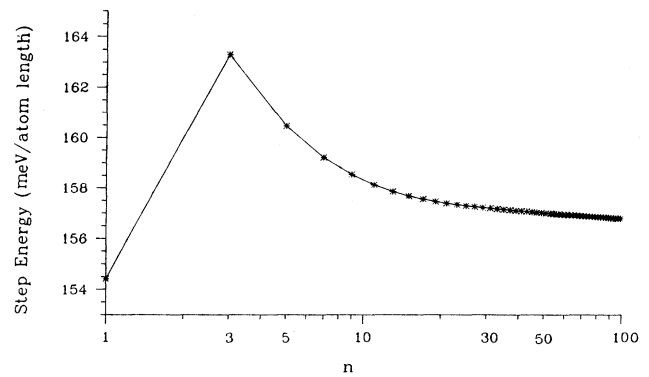

FIG. 3. The calculated ledge energy per atom length $\lambda(d)$ vs n. Note that the step width $d = n/2$ and that the abscissa is on a logarithmic scale.

the surface energies are summarized in Table I, together with the results[15,19,20,23] of other computations as well as experimental data.[21] Our results compare well with others in the table. As can also be seen, the surface energies obtained from the newer equivalent crystal theory[19] give better agreement with experimental data.[21] Since the experimental values are obtained for an average face, this comparison is only of qualitative interest.

Figure 3 displays the step excess energies obtained from Eq. (2) as a function of step spacing (the terrace width $d = n/2$). A least-squares fit to the step energies of the vicinal surface $(1,1,2m+1)$ for $m = 5$–49 times

$$\lambda(d) = 0.1569 + 0.0827/d^{2.2327} , \qquad (4)$$

thus indicating an isolated ledge energy λ_0 of 0.1569 eV (1821 K) per ledge atom. The elastic repulsive step-step interaction energy is shown in Fig. 3 to be long ranged, and to begin even at the short range of the (1,1,3) vicinal

surface. The dependence of λ on d in Eq. (4), for large values of d, is reasonably close to d^{-2}, as expected from the elasticity theory.

As a test of the EAM potential, we have also calculated the step-step interaction ω_5 for Cu(1,1,5) following the definition in Ref. 15, i.e., one column of atoms at the ledge positions was removed from the upper surface of the slab and attached to the lower one. The energy difference between this system and the clean one gives a repulsive ω_5 of 13 K in our calculations. This value is lower than that of 100 K, which was estimated from experimental data[22] analyzed assuming repulsive elastic interaction between steps. Our calculated value for ω_5 has the same sign as that extracted from the data, in contrast to a negative (attractive) value computed by Liosel et al.[15]

It is interesting to look at the characteristic excess energies of various types of atoms on the puckered layer. This layer is shown in Fig. 4, starting from the right at the ledge, moving under the next ledge, and so on. Here the side view of some $(1,1,n)$ surfaces is given, with S denoting atoms at step edges, T the terrace atoms, C the corner atom representing the boundary between two terraces, and, finally, B representing bulklike atoms.

As shown in Fig. 5, an S atom at the ledge has the highest energy of 0.67 eV, due to its lowest coordination numbers, i.e., seven nearest neighbors (7NN). A terrace atom with 8NN has an energy of 0.48 eV, and a corner atom with 10NN an energy of 0.25 eV. The atoms under the next ledge with 12NN lose only their next-nearest neighbors, and the excess energies are less than 0.04 eV.

B. Step-pair interactions

In consideration of step meandering,[2,5] or reconstruction of stepped surfaces,[8,13] information on step-pair interactions is needed. The elastic step excess energy described in Sec. III A, calculated with periodic surface unit cells, is automatically a sum of all step-step interaction energies, with separation varying as integral multiples of the terrace width. To calculate the step-pair interaction as defined earlier, we need to isolate the step-step interaction for a given separation. Of course, for higher-index
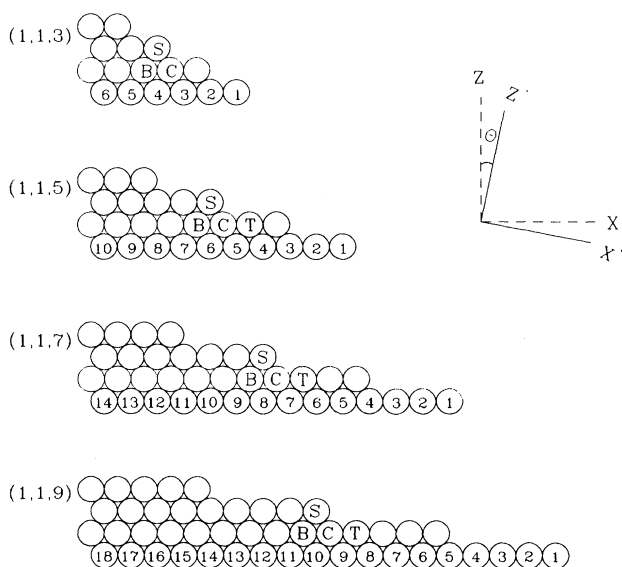
TABLE I. Comparison of the surface energies of the relaxed $(1,1,n)$ surfaces at $T = 0$ K. Units are in erg/cm^2.

	(100)	(111)	(113)	(115)	(117)
Present work	1288	1181	1406	1391	1372
Loisel et al.[a]	1345	1240	1455	1446	
Sinnott et al.[b]	1640	1510	1750		
Lin et al.[c]	1321	1215	1443		
Smith and co-workers[d]	2380	1830			
Experimental		1790[e]			2016[f]

[a]Reference 15.
[b]Reference 20.
[c]Reference 23.
[d]Reference 19.
[e]Reference 21(a).
[f]Reference 21(b).

FIG. 4. The side view of the $(1,1,n)$ surfaces. Here S denotes a ledge atom, T a terrace atom, C a corner atom, and B a bulk-like atom. Note the numbering of the layers on stepped surfaces. The flat surface coordinates are defined such that the [110] direction is the x axis and [001] is the z axis. The stepped surface coordinates can be obtained by rotating the x and z axes by a tilt angle θ.

vicinal surfaces which have large step separations, a nearest-neighbor pair interaction between steps is equivalent to a ledge-ledge interaction since the long-range step interaction over two terrace widths is negligible. However, as the step separation is reduced, we are no longer in the elastic limit and the ledge-ledge interaction is no longer equivalent to a nearest-neighbor step-pair interaction. We discuss below a method for extract-
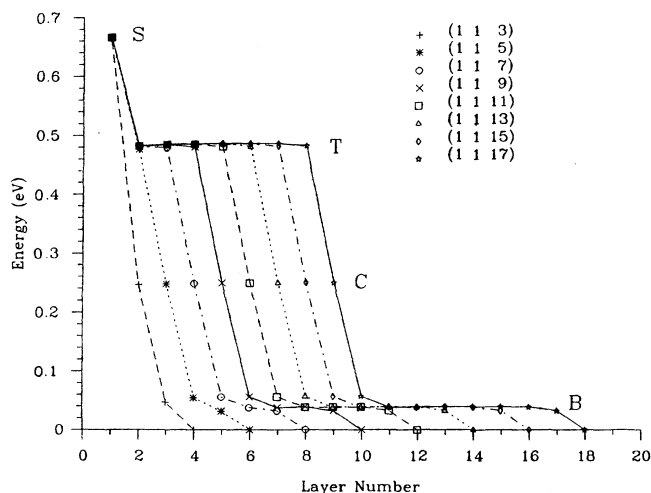
ing a step-pair interaction for two steps at short separations.

We begin with a 2×4 surface cell of the $(1,1,99)$ vicinal, for which the ledge energy is seen to be very close to the isolated step energy λ_0 (see Fig. 3). The atoms located on one terrace were removed column by column (along the step direction) and attached to the opposite surface, creating a $(1,1,2m+1)$ facet, with m varying from 1 to 12 on both sides of the slab. The pair interaction energy $\lambda_{(m+1/2)}$ is given by

$$\lambda_{(m+1/2)} = (E_{(1,1,2m+1)} - E_{(1,1,99)})/(2L_y) , \qquad (5)$$

where $E_{(1,1,2,+1)}$ is the total energy of the system consisting of the $(1,1,2m+1)$ facets, $E_{(1,1,99)}$ the total energy of the clean surface, L_y the length along the step direction in the unit cell, and the factor of 2 taking into account the two free surfaces.

Figure 6 shows the calculated step-pair interaction versus the microfacet index $2m+1$ for the $(1,1,2m+1)$ facets, with $m=1-12$. The curve converges to the ledge-ledge interaction energy curve in Fig. 3 for $m \geq 13$. On comparing, one can distinguish the step-pair interaction from the ledge-ledge interactions. Again, the step-pair interaction also has the repulsive elastic interaction, just like the ledge-ledge interaction.

C. Kink-formation energy

The kink-formation energy was calculated on $(1,1,5)$ and $(1,1,29)$ vicinals with 4×12 and 2×12 surface super-cells, respectively, in order to make a comparison of the effect of step spacing. The kinks were created without changing the total number of atoms by removing six atoms along one step ledge of the upper surface and attaching them to one step edge of the lower surface so that the system contains four kinks. The calculated kink-formation energy for $(1,1,5)$ is 1570 K (0.1353 eV), while that for $(1,1,29)$ is 1587 K (0.1368 eV). The effect of increasing the terrace width is thus to increase slightly the kink-formation energy. Our calculated result can be
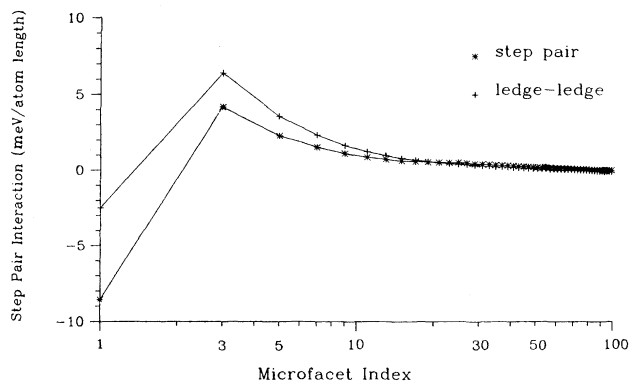

FIG. 5. The excess energy distributions for atoms on stepped surfaces where the layer number and the atom label S, T, C, and B are as in Fig. 4.

FIG. 6. Step-pair interactions vs $2m+1$ of $(1,1,2m+1)$ facets, with $m=1-12$. The curve converges to the ledge-ledge interaction as $m \geq 13$. The ledge-ledge interaction (subtracting the isolate step energy from Fig. 3) is also shown for comparison.

compared with the kink-formation energy 1412 K for (1,1,5) by Loisel *et al.*[15] The experimental data on Cu(100) suggest a much lower kink-formation energy of 1165 K.[10]

The multiple-kink energy $E(n)$, with a length of n kinked atoms, was calculated on (1,1,29). The results can be well fitted by

$$E(n) = n\epsilon_k + 2\epsilon_c ,\qquad (6)$$

with the kink-formation energy ϵ_k of 0.159 eV (1845 K) and a corner energy ϵ_c of -11.3 meV (-131 K). The corner energy introduced can be thought of as corresponding to the additional attractive energy due to the existence of two corners of a kink. The kink-formation energy ϵ_k is seen to be close to the isolated ledge energy λ_0 in Eq. (4). This is easy to understand since the ledge and kink atoms have the same coordination numbers, except for those atoms which are located at the corners of a multiple-length kink.

D. Activation energies of adatoms diffusing on stepped surfaces

All the calculated activation energies E_d were obtained for the (1,1,7) surface. The results are displayed in Table II for the different cases of adatoms or kinked atoms diffusing on the surface. For an adatom diffusing between two adjacent terrace sites, the calculated E_d is 0.49 eV, which is to be compared with the results[23] using the two different sets of EAM potentials on a clean Cu(100) surface, a value of 0.38 eV with a set developed by Adams, Foiles, and Wolfer (AFW) (Ref. 24), and a value of 0.53 eV obtained by Voter and Chen (VC).[25]

The 0.26-eV diffusion barrier of an adatom along the step direction, as shown in Fig. 7(a), can be compared with that of 0.26 (AFW) and 0.28 eV (VC) on a Cu(1,1,3) surface.[23] The evaporation of an atom incorporating at the step edge onto a free terrace site needs to overcome a barrier of 0.83 eV, and an inverse process meets a barrier of only 0.46 eV. On the other hand, an adatom created from a kink site along a step edge has an activation energy of 0.53 eV, and an inverse process meets a barrier of 0.23 eV. The two processes are schematically shown in Fig. 7(b). In addition, a vacancy in a step diffusing along the step direction [see Fig. 7(e)] has an energy barrier of 0.49 eV. From these values, we can conclude that an

TABLE II. Activation energies of adatoms diffusing on a (1,1,7) surface. Energies are in eV.

On the terrace	0.49
Along the step edge	0.26
Away from step edge onto terrace	0.83
From terrace to step edge	0.46
From kink site along step edge	0.53
From step edge to a kink site	0.23
From kink edge onto terrace	0.56
Vacancy in a step	0.49
Jump from terrace into descending step	0.79
Exchange with an edge atom	0.50

◯ atoms of lower terrace	⊕ atoms of upper terrace	● adatoms
(a)	(b)	(c)

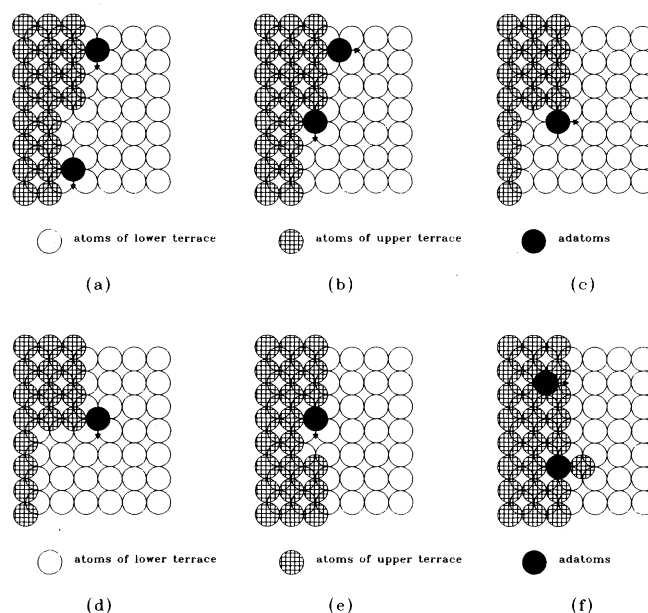|		
◯ atoms of lower terrace	⊕ atoms of upper terrace	● adatoms
(d)	(e)	(f)

FIG. 7. Top views of the possible adatom diffusion paths on the (1,1,7) surface. Arrows in (a)–(f) indicate adatom jump directions. The adatom diffusions are displayed in (a) along the step direction; (b) away from the step edge onto the terrace and from the kink site along the step edge; (c) and (d) from the kink edge onto the terrace; (e) the vacancy along the step direction; and (f) the jump from the terrace into the descending step and the exchange with an edge atom.

adatom near a step edge has much higher mobility along the step direction than that of a motion normal to the step. The relative magnitudes of the activation energies of adatoms moving along and normal to the step direction in our calculations is in accord with those used to interpret the frizzled step behavior in the recent STM experiments.[10,11]

The evaporation barrier for an adatom from the step edge onto the terrace sites may be lowered as the environment of the adatom changes. As given in Table II and shown in Fig. 7(c), an adatom at the end of a multiple-length kink site, or, as in Fig. 7(d), one in front of a kink site with 5NN, experiences a barrier of 0.56 eV when it diffuses onto a terrace site indicated by the arrow in Fig. 7(c) or 7(d). It can be expected from this significant reduction of the barriers that, as the number of kinks increases with increasing substrate temperature, more mobile adatoms along the step may be evaporated onto the terrace from the vicinity of the outermost ends of the kinks.

The surface adatom diffusion may be completed with an exchange process, in which the adatom replaces a substrate atom along the [100] direction, rather than a simple bridge-site jump along [110], which was recently proposed by Feibelman[26] for fcc(100) and observed in experiments.[27] For Cu self-diffusion on (100) with this mechanism, activation barriers of 0.72 (AFW) and 0.79 eV (VC) were obtained,[23] which is much higher than that of a simple bridge-jump model. Our calculations showed that

E_d^{ex} is even higher than 1.0 eV on the (1,1,7) terrace. It seems unlikely from our calculations that the exchange diffusion is favorable on these terrace sites.

The exchange process is energetically preferable, however, for an adatom jumping into a descending step, as can be read from Table II. In a simple bridge-jump diffusion, where the adatom diffusion direction is displayed in the upper part of Fig. 7(f), the activation barrier is about 0.79 eV. However, in an exchange process, where the adatom exchanges place with an adjacent atom in the step edge and eventually that edge atom becomes an adatom along the step, as shown in the lower part of Fig. 7(f), the barrier was calculated to be 0.5 eV, comparable to that of an adatom diffusing on the free surface. This result is very intriguing, as the step edge was believed to be a strong repulsive potential barrier preventing the adatom from moving down to the next terrace. Our calculated result confirms the possible potential curve for an adatom moving toward a step with an exchange process proposed by Wang and Ehrlich in a recent field-ion-emission experiment.[28]

E. Surface relaxations

We have also obtained the values of the interlayer relaxations on stepped surfaces. The outmost surface layer is labeled as the first layer and, as described in Fig. 4, the layer number increases as one goes into the bulk. Note that for a stepped surface, interlayer spacing as defined above is a small quantity, decreasing in magnitude with increasing terrace width. The percentage interlayer relaxation $d_{i,i+1} = 100[(z_i' - z_{z+1}') - z_0']/z_0'$ is a measure of the deviation of the interlayer distance $(z_i' - z_{i+1}')$ from the unrelaxed bulk value of $z_0' = \sin\theta$. Figures 8 and 9 illustrate the percentage relaxations $d_{i,i+1}$ of $\mathrm{Cu}(1,1,2m+1)$, with $m = 1-8$. From these figures, we see that the maximum relaxations occur at the vicinity of the step-edge positions. The following remarks can also be deduced from the figures:

(a) The inward relaxation of the outermost surface planes holds for all vicinal surfaces. This general features has been well established by experiments[29-32] and by theoretical calculations,[15,24,33,34] and it may be argued
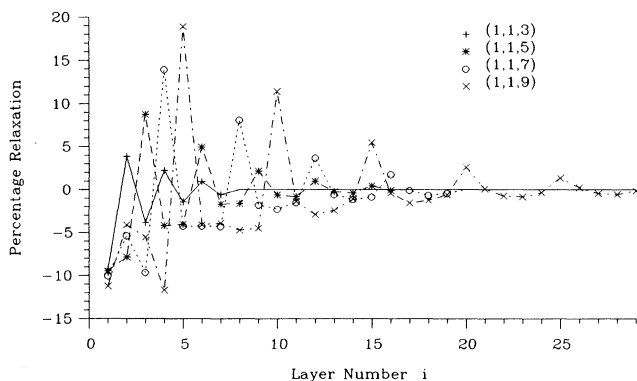

FIG. 8. Percentage relaxations of (1,1,3), (1,1,5), (1,1,7), and (1,1,9).
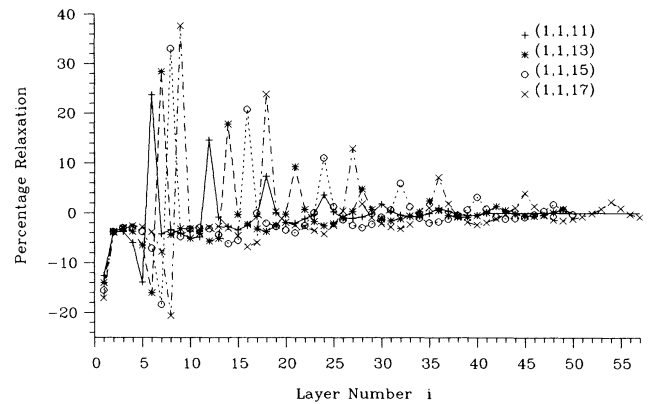

FIG. 9. Percentage relaxations of (1,1,11), (1,1,13), (1,1,15), and (1,1,17).

qualitatively that an atom in the first layer seeks an environment of higher electron densities in order to gain a higher binding energy, and as a consequence, the distance between the first and second layers is shortened.

(b) The magnitude and range of the oscillatory relaxations near the free surfaces appear to increase with increasing size of the planar unit cell, i.e., increasing the number m for the $(1,1,2m+1)$ surfaces. Such a tendency has been realized both experimentally[29,35] and theoretically.[15,34] This observation does not mean that the displacements of surface atoms are larger for more rough surfaces; rather that they are an artifact of the definition of $d_{i,i+1}$. This may be illustrated by the following consideration. Suppose that two nearest-neighbor atoms located along a terrace belong to two adjacent atomic layers as defined in Fig. 4. With the full relaxation of all atoms of the system, the relative displacement of these two atoms is measured in the flat surface coordinates (xyz) of Fig. 4 to be $\delta\mathbf{r}_{i,i+1} = (1+\Delta x_{i,i+1})\mathbf{i} + \Delta z_{i,i+1}\mathbf{k}$ (where $\Delta y_{i,i+1} = 0$ due to the symmetry along the step direction). The projection of this displacement along the $(1,1,2m+1)$ surface normal, as measured in the surface coordinates $(x'y'z')$ (see also Fig. 4), is

$$\Delta z_{i,i+1}' = (1+\Delta x_{i,i+1})\sin\theta + \Delta z_{i,i+1}\cos\theta . \qquad (7)$$

Then the percentage of the displacement δd defined in the above can be written as

$$\delta d_{i,i+1} = \Delta x_{i,i+1} + \frac{(2m+1)\Delta z_{i,i+1}}{\sqrt{2}} , \qquad (8)$$

which is proportional to the number $(2m+1)$. This simple relation is valid for all $\delta d_{i,i+1}$, as can be seen from Figs. 8 and 9, in which the relaxation values of each corresponding site (edge atoms S, terrace atoms T, corner atoms C, and bulk atoms B in Fig. 4) do hold straight lines, and each of their slopes presents a displacement of adjacent two layers along the z-[001] direction. The perfect linear relation of each corresponding relaxation between $(1,1,2m+1)$ vicinal surfaces implies that the displacements of each atomic layer in one vicinal remain almost unchanged in the corresponding sites on an another vicinal surface.

(c) The relaxations for a given vicinal $(1,1,2m+1)$ away from the surface show an oscillatory character with a periodicity of $m+1$ layers and an exponential damping in magnitudes. Such an asymptotic behavior was studied theoretically some time ago,[36,37] and was shown to be related to the bulk phonon dispersion in the complex wave-vector plane. Our results give a quantitative confirmation of the earlier predictions on realistic metal surfaces. Numbers taken from Figs. 8 and 9 for interlayer relaxation follow the exponential law

$$\delta d_{l(m+1)+i,l(m+1)+i+1} = \delta d_{i,i+1}\exp[-K_i(l-1)] , \qquad (9)$$

where $l=1,2,\ldots$ indicates the periodicity of the relaxation. For the maximum relaxations at sites $l(m+1)$ $(l=1,2,\ldots)$, the values of K were found to be in a range of $0.47\sim0.40$ for $m=1-8$. The slight m dependence of K on m can be understood from Eq. (8). In the Appendix, a simple force-constant model is given for the analysis of surface relaxations. The main features of the above numerical results for the relaxations can be well reproduced.

These $m+1$ periodicity and exponential decaying properties of the multilayer relaxations call for future experimental confirmation.

IV. DISCUSSIONS

As mentioned in the Introduction, the main motivation of this work was to obtain information about the step-step interaction on stepped surfaces. The results given in Sec. III show that the static interaction between steps at different separations corresponds to the elastic repulsion, in agreement with the elasticity theory. It is clear that this elastic interaction cannot explain the attractive forces between steps at intermediate atomic distances, as found in STM experiments.[9−11] The possible sources of the attractive forces may be due to other types of interaction,[4,9] such as an indirect electron interaction between steps. For adatoms on metal surfaces, these interaction energies were evaluated to be much smaller than the elastic energy. On stepped surfaces, all the above-mentioned interactions between steps are parts of the free energy. Another significant contribution to the lattice free energy is the phonon energy, which has not been considered in the existing literature on step interactions, to our knowledge. We would like to suggest that the inclusion of phonon energy may be very crucial to the understanding of the step free energy and hence surface morphology. This point may be inferred from the following considerations: (1) the magnitude of the step-step interaction energy is several meV, which is comparable to the phonon energy of atoms. Therefore quantum correction from zero-point motion should be included in the free energy of the system; and (2) presence of step phonon[38] will lower the surface-phonon excess energies as compared to those of a flat surface. Since the $(1,1,n)$ vicinal surfaces with lower n have the higher step densities, they are expected to possess lower vibrational excess energies. An explicit calculation taking into account the phonon contribution to the stepped surface free energy is underway.

The necessity of using a many-body potential is essential in obtaining the surface excess energies. This point is evidenced in the kink-formation energy calculation for which an EAM value of 1570 K is comparable to the experimental[10] one of 1165 K, whereas the bond-breaking model gives a value of 3400 K.[4] With EAM potentials, we have also obtained the step-step elastic interactions, in contrast to a negative value calculated for $Cu(1,1,5)$ from another semiempirical many-body potential.[15]

It should be emphasized that the ledge-ledge interaction, being, in general, a sum of all pair interactions of steps deviates from a single-step-pair interaction energy for short ledge separations of vicinal surfaces. We have calculated the step-pair interaction in order to identify this difference. The step-pair interaction is very important in obtaining the stepped surface morphology.[5] It is our hope that these calculated interaction functions can be used in further thermodynamic simulations of stepped Cu surfaces.

As a final point, we should mention that the activation energies calculated in Table II, for adatoms diffusing on the stepped and kinked surfaces, are in reasonable agreement with other EAM-type computations. One interesting result is that the exchange process may occur at the step ledge as an adatom incorporates to the descending step. On the other hand, the exchange diffusion is predicted to be of higher activation energy than that of a simple bridge jump on the terrace. Our EAM result is in disagreement with a recent effective-medium-theory (EMT) calculation[39] where the ordinarily used EMT potential for Cu was corrected by including the one-electron energy term. In the calculations of Ref. 39, a value of 0.22 eV for the exchange activation energy on $Cu(100)$ was obtained which is much lower than a bridge-jump value 0.43 eV and is in excellent agreement with the experimental value of 0.28 eV.[40] The discrepancy between the corrected EMT result[39] and the present one, as well as other EAM results,[22] implies that there are still some inherent features of the present EAM version that are unable to reproduce some of the experimental phenomena, such as exchange diffusion on $Cu(100)$.

APPENDIX A: FORCE-CONSTANT MODEL FOR SURFACE RELAXATIONS

It was pointed out[37] that the multilayer relaxation is related to the zero-frequency solution in the complex phonon structure. It is our purpose here to extend the discussion of the elastic vibrations of crystal surfaces to the present system. To simplify the problem, we suppose that the planes of atoms are displaced as a whole parallel or perpendicular to the surface normal and that all planes of atoms are identical. The displacement of the plane s

TABLE III. Zero roots of photon frequencies with complex wave vectors for $(1,1,2m+1)$, with $m=1-8$ in a nearest-neighbor force-constant model.

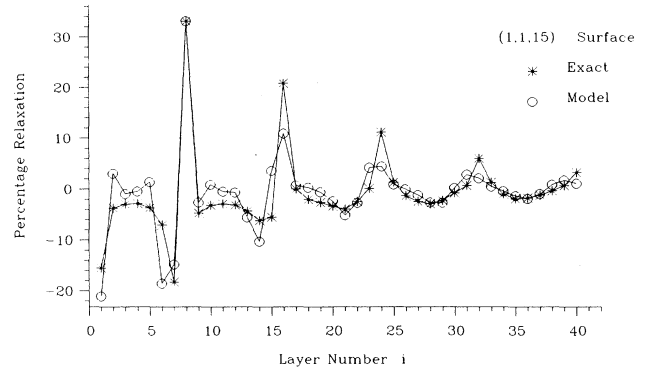|	
(1 1 3)	$3.142+i0.603$
(1 1 5)	$2.172+i0.397$
(1 1 7)	$1.666+i0.241$
	$3.142+i0.410$
(1 1 9)	$1.338+i0.153$
	$2.585+i0.322$
(1 1 11)	$1.111+i0.104$
	$2.187+i0.229$
	$3.142+i0.322$
(1 1 13)	$0.948+i0.074$
	$1.882+i0.164$
	$2.751+i0.269$
(1 1 15)	$0.826+i0.056$
	$1.645+i0.121$
	$2.436+i0.206$
	$3.142+i0.269$
(1 1 7)	$0.731+i0.044$
	$1.459+i0.093$
	$2.174+i0.156$
	$2.840+i0.232$

FIG. 10. The plot of the asymptotic relaxations (model) of $(1,1,15)$ from a force-constant model. The numerical results (exact) from the EAM calculation are also shown for comparison.

from its bulk position is described by a single coordinate u_s. The elastic energy of the system can then be written as

$$E = -\sum_s F_s u_s + \tfrac{1}{2}\sum_{s,p} C_{sp} u_s u_p \ , \tag{A1}$$

where F_s is the total force on plane s and C_{sp} is the planar force constant between planes s and p. The relation between F_s and C_{sp}'s is of the form of Hooke's law.[41]

$$F_s = \sum_p C_{sp}(u_{s+p} - u_s) \ . \tag{A2}$$

The stable positions u_s are thus given by the above equation. F_s are nonzero in the vicinity of the surface, and vanish away from the source, and consequently C_{sp}'s tend to C_{sp}^{p0}, the bulk planar force constants. Therefore the asymptotic form of Eq. (A2) away from the surface is just related to the solutions of the zero vibrational frequency, with complex wave vectors along the surface normal which describe the reconstruction or relaxation of the surface.[36,37]

If we make the further approximation that interactions only among nearest-neighbor atoms are important, the bulk phonon dispersion in the $(1,1,2m+1)$ surface coordination system reads

$$\frac{M}{2}\omega^2 = C_1(1-\cos\alpha) + C_m[1-\cos(m\alpha)]$$

$$+ C_{m+1}\{1-\cos[(m+1)\alpha]\} \ , \tag{A3}$$

where M is the mass of atoms and $\alpha = (k_\perp + iK)a_s$, with the perpendicular complex wave vector $(k_\perp + iK)$ and a_s the bulk planar distance along the surface direction. The planar force constants $C_p (=C_{s,s+p}$, with $p \geq 1)$ are given in terms of only one atomic force constant β, and the second derivative of the two-body interaction between

two atoms evaluated at their equilibrium positions is as follows:

$$C_1 = \beta \sin^2\theta \ , \tag{A4a}$$

$$C_m = \frac{\beta}{2}[1 + \cos^2\theta - \sqrt{2}\sin(2\theta)] \ , \tag{A4b}$$

$$C_{m+1} = \frac{\beta}{2}[1 + \cos^2\theta + \sqrt{2}\sin(2\theta)] \ . \tag{A4c}$$

The asymptotic behavior u_s corresponds to a combination of bulk zero frequencies in Eq. (A1), and is written as

$$u_s = \sum_{\omega_i(\alpha)=0} C_{\omega_i} N_{\omega_i} \exp[-(s-1)K_i]\cos(sk_\perp^i a_s + \phi_{\omega_i}) \ , \tag{A5}$$

where C_{ω_i} is the coefficient to be determined and N_{ω_i} is the normalization factor of an eigenvector. Solving for the zero roots of Eq. (A3) for the $(1,1,3)$ surface, we obtain the displacements of the form of Eq. (7):

$$u_s = u_0(-1)^s \exp[-(s-1)K] \ , \tag{A6}$$

where $K = \cosh^{-1}(1 + 3C_1/2C_2)$, with C_1 and C_2 given in Eq. (A4). The coefficient u_0 can be determined by matching the value to the force acting on the first layer through Eq. (A2). In the $(1,1,3)$ situation, $K = 0.60$ is evaluated by Eq. (A6), which can be compared to the numerical calculated value of 0.47.

In Table III, we present the calculated roots of the zero solutions of α in Eq. (A3) for the vicinal surface $(1,1,2m+1)$, with $m=1-8$. As an example, we give the results of $(1,1,15)$ with four zero roots (see Table III) in Fig. 10. It can be seen clearly that even without the knowledge of atomic force constant β in solving Eq. (A3), the main features started in Sec. III E for the relaxations can be reproduced by the simple model above. Of course, a quantitative evaluation of the relaxations needs to take into account interaction with additional neighbors and more accurate atomic potentials for improving the above analytical model.

*Present address: Physics Department, Brock University, St. Catharines, Ontario, Canada L2S 3A1.

[1]C. Herring, Phys. Rev. **82**, 87 (1951).

[2]W. K. Burton, N. Cabrera, and F. C. Frank, Philos. Trans. R. Soc. London **243A**, 299 (1951).

[3]For a review, see J. D. Weeks, in *Ordering in Strongly Fluctuating Condensed Matter Systems*, edited by T. Riste (Plenum, New York, 1980), p. 293.

[4]J. Villian, D. R. Grempel, and J. Lapujoulade, J. Phys. F **15**, 809 (1985).

[5]N. Bartelt, T. L. Einstein, and E. D. Williams, Surf. Sci. Lett. **240**, L591 (1990).

[6]R. Kariotis and M. G. Lagally, Surf. Sci. **248**, 295 (1991).

[7]X. S. Wang, J. L. Goldberg, N. C. Bartelt, T. L. Einstein, and E. D. Williams, Phys. Rev. Lett. **65**, 2430 (1990).

[8]B. S. Swartzentruber, Y.-W. Mo, R. Kariotis, M. G. Lagally, and M. B. Webb, Phys. Rev. Lett. **65**, 1913 (1990).

[9]J. Frohn, M. Giesen, M. Poensgen, J. F. Wolf, and H. Ibach, Phys. Rev. Lett. **67**, 3543 (1991).

[10]M. Poensgen, J. F. Wolf, J. Frohn, M. Giesen, and H. Ibach, Surf. Sci. (to be published).

[11]M. Giesen, J. Frohn, M. Poengsgen, J. F. Wolf, and H. Ibach, J. Vac. Sci. Technol. (to be published).

[12]J. Wintterlin, R. Schuster, D. J. Coulman, G. Ertl, and R. J. Behm, J. Vac. Sci. Technol. B **9**, 902 (1991).

[13]T. W. Poon, S. Yip, P. S. Ho, and F. F. Abraham, Phys. Rev. Lett. **65**, 2161 (1990).

[14]A. Bartolini, F. Ercolessi, and E. Tosatti, Phys. Rev. Lett. **63**, 872 (1989).

[15]B. Loisel, D. Gorse, V. Pontikis, and J. Lapujoulade, Surf. Sci. **221**, 365 (1989).

[16]M. S. Daw and M. I. Baskes, Phys. Rev. B **29**, 6443 (1984); S. M. Foiles, M. I. Baskes, and M. S. Daw, *ibid.* **33**, 7983 (1986).

[17]R. Nelson, Master's thesis, University of Maryland, 1991. This work reports studies on stepped Ag(111) surfaces.

[18]W. K. Rilling, C. M. Gilmore, T. D. Andreadis, and J. A. Spragne, Can. J. Phys. **68**, 1035 (1990).

[19]J. R. Smith and A. Banerjea, Phys. Rev. Lett. **59**, 2451 (1987). For more detail about the equivalent crystal theory, see J. R. Smith and A. Banerjea, Phys. Rev. B **37**, 10411 (1988); J. R.

Smith, T. Perry, A. Banerjea, J. Ferrante, and G. H. Bozzollo, *ibid.* **44**, 6444 (1991).

[20]S. B. Sinnott, M. S. Stave, T. J. Raeker, and A. E. DePristo, Phys. Rev. B **44**, 8927 (1991).

[21](a) W. R. Tyson and W. A. Miller, Surf. Sci. **62**, 267 (1977); (b) H. Wawra, Z. Metallk. **66**, 395 (1975); **66**, 492 (1975).

[22]F. Fabre, D. Gorse, B. Salanon, and J. Lapujoulade, J. Phys. (Paris) **48**, 1017 (1987).

[23]C. Liu, J. M. Cohen, J. B. Adams, and A. F. Voter, Surf. Sci. **253**, 334 (1991).

[24]J. B. Adams, S. M. Foiles, and W. G. Wolfer, J. Mater. Res. **4**, 102 (1989).

[25]A. F. Voter and S. P. Chen, in *Characterization of Defects in Materials*, edited by R. W. Siegel, J. R. Weertman, and R. Sinder, MRS Symposia Proceeding No. 82 (Materials Research Society, Pittsburgh, 1987), p. 175.

[26]P. J. Feibelman, Phys. Rev. Lett. **65**, 729 (1990).

[27]G. L. Kellogg and P. J. Feibelman, Phys. Rev. Lett. **64**, 3134 (1990); C. L. Chen and T. T. Tsong, *ibid.* **64**, 3147 (1990); G. L. Kellogg, Surf. Sci. **246**, 31 (1991).

[28]S. C. Wang and G. Erlich, Phys. Rev. Lett. **67**, 2509 (1991).

[29]P. R. Watson and K. A. R. Mitchell, Surf. Sci. **203**, 323 (1988).

[30]H. L. Daries and J. R. Noonan, Surf. Sci. **126**, 245 (1983).

[31]S. A. Lindgren, J. Wallden, J. Rundgren, and P. Westrin, Phys. Rev. B **29**, 576 (1984).

[32]M. Copel, T. Gustafsson, W. R. Graham, and S. M. Yalisove, Phys. Rev. B **33**, 8110 (1986).

[33]T. Ning, Q. Yu, and Y. Ye, Surf. Sci. **206**, L857 (1988).

[34]D. Wolf, Surf. Sci. **226**, 389 (1990).

[35]M. A. Van Hove, in *The Nature of the Surface Chemical Bond*, edited by T. W. Rhodin and G. Ertl (North-Holland, Amsterdam, 1979).

[36]G. Allen and M. Lannoo, Surf. Sci. **40**, 375 (1973); Phys. Status Solidi B **74**, 409 (1976).

[37]G. Allen and M. Lannoo, Phys. Rev. B **37**, 2678 (1988).

[38]P. Knipp, Phys. Rev. B **43**, 6908 (1991).

[39]L. Hansen, P. Stoltze, K. W. Jacobsen, and J. K. Nørskov, Phys. Rev. B **44**, 6523 (1991).

[40]See Ref. 39, *Note added in proof*.

[41]C. Kittel, *Introduction to Solid State Physics*, 5th ed. (Wiley, New York, 1976).